Peer reviewed version

Link to published version (if available):
10.1002/joc.6094

Link to publication record in Explore Bristol Research
PDF-document

University of Bristol - Explore Bristol Research
General rights

International Journal of Climatology

RMetS
Royal Meteorological Society

Spatio-temporal drought patterns of multiple drought indices based on precipitation and soil moisture: A case study in South Korea

SCHOLARONE™
Manuscripts

1 **Spatio-temporal drought patterns of multiple drought indices based on precipitation**

2 **and soil moisture: A case study in South Korea**

3 *Spatio-temporal drought patterns of multiple drought indices*

4 Moonhyuk Kwon[1], Hyun-Han Kwon[2, *] and Dawei Han[1]

5 Civil and Environmental Engineering, University of Bristol, United Kingdom

6 Department of Civil and Environmental Engineering, Sejong University, Seoul, South Korea

7 (***Contact:** *hkwon@sejong.ac.kr*)

8

9 **Abstract**

10 This study aims to explore the spatio-temporal characteristics of meteorological and

11 agricultural droughts using the Standardized Precipitation Index (SPI) and Standardized Soil

12 Moisture Index (SSI), respectively, as well as their relationships over the past three decades

13 (1986-2016) in South Korea. The SSI shows less frequent droughts and longer drought

14 duration compared to the SPI, due to the gradual decrease in the autocorrelation functions of

15 the SSI. The strongest cross-correlations are observed at a 1-month lag between the SPI and

16 SSI for most stations. Thus, the SPI could be more appropriate for defining the onset of a

17 drought, whereas the SSI appears to be more effective for describing drought persistence.

18 Moreover, the transition from meteorological to agricultural droughts is significantly

19 dependent on the season, indicating that the transition between them is highly correlated with

20 antecedent moisture conditions. The copula-based Multivariate Standardized Drought Index

21 (MSDI) is introduced to explicitly postulate interdependence between the SPI and SSI in the

22 context of a multivariate probability distribution. We employ a hierarchical agglomerative

23 clustering approach along with a quantile regression model to better understand the spatio-

24 temporal pattern of the MSDI. More drought episodes under moderate to severe drought

25 conditions are observed along the southern coast of South Korea. Additionally, persistent

26 droughts with higher severity are observed in the northern part of South Korea, which may be

27 attributed to a significant decreasing trend (or increasing drought risk).

28 **Keywords:** SPI, SSI, Multivariate drought index, Clustering analysis, Quantile regression

29

30 **1. Introduction**

31 Drought is a periodic phenomenon that exerts multifaceted negative impacts on a wide range

32 of water-related sectors, which can eventually lead to severe direct (or indirect) socio-

33 economic losses (Mckee et al. 1993; Spinoni et al. 2014; Vidal et al. 2009). Droughts occur

34 virtually everywhere in the world, but their characteristics, such as duration, intensity and

35   frequency, vary significantly depending on climate zones (Mirabbasi et al. 2013).

36   Additionally, it is expected that climate change will accelerate changes in drought

37   characteristics (Dai 2011; Van Loon et al. 2016). Thus, drought monitoring and early warning

38   systems at global and local scales have emerged as powerful platforms for preventing and

39   mitigating the negative effects of drought.

40   Drought is rather different from other water related hazards in terms of its spatio-temporal

41   characteristics, resulting in structured spatial coverage with varying durations. Moreover, the

42   spatio-temporal drought patterns may differ substantially by drought intensity. In these

43   contexts, an exploration of the spatio-temporal drought patterns over different quantiles (i.e.

44   severity) can serve as a basis to understand the evolution and nature of droughts in space and

45   time. However, most of existing studies on droughts have not specifically analyzed the

46   spatio-temporal patterns at different quantiles. Thus, this study will focus on exploring the

47   underlying structure of drought occurrence and development.

48   Many studies have been conducted to estimate the onset, persistence and termination of

49   drought events using meteorological and hydrological variables (Ganguli and Ganguly, 2016;

50   Mo, 2011; Shukla et al., 2011; among others). Drough features such as duration, severity and

51   intensity are commonly characterized by drought indices, which provide a more

52   comprehensive perspective for drought monitoring and management compared to the direct

53   use of hydro-meteorological variables (e.g., precipitation, soil moisture (SM) and streamflow)

54   (Zargar et al. 2011). Nonetheless, the selection of the drought index for a certain purpose

55   remains controversial (Farahmand & AghaKouchak 2015). Specifically, the identification of

56   drought can be attributed to the choice of drought index that, with some limitations,

57   incorporates different aspects of drought conditions (Hao & Singh 2015). Accordingly,

58   various drought indices have been proposed to detect different types of droughts. For

59   example, a meteorological drought index refers to deficits in precipitation and/or evaporation,

60   whereas agricultural and hydrological drought indices are based on deficits in SM and

61   streamflow, respectively (Dracup et al. 1980).

62   The drought indices are mainly used to describe different types of droughts (i.e.

63   meteorological, agricultural, hydrological, and socioeconomic droughts). They are commonly

64   derived from a single hydrological variable (e.g., rainfall: the standardized precipitation index

65   (SPI), and standardized anomaly index (SAI), streamflow: standardized streamflow index

66   (SSI) and streamflow drought index (SDI), groundwater: standardized water-level index

67   (SWI) and soil moisture: Standardized soil moisture index (SSI)). On the other hand, there

68   are several examples that combine two or more variables such as the Palmer drought severity

69   index (PDSI; Palmer, 1965), standardized precipitation evapotranspiration index (SPEI;

70   Vicente-Serrano et al., 2010), surface water supply index (SWSI; Shafer and Dezman, 1982)

71   and multivariate standardized drought index (MSDI; Hao and AghaKouchak, 2013). Here, we

72   only introduced some of the drought indices, and would suggest that for more details readers

73   are kindly referred to Svoboda and Fuchs (2017). Among many drought indices, the SPI,

74   proposed by Mckee et al., (1993), has been widely adopted as a tool for monitoring long-term

75   drought conditions at multiple time scales. More specifically, the advantage of the SPI

76   method lies in its relative simplicity of computation and ease of interpretation, and the SPI

77   approach is particularly useful in predicting drought onset (Hao & AghaKouchak 2013).

78   Thus, the World Meteorological Organization (WMO) endorsed the SPI as a standard

79   drought indicator (Hayes et al. 2011). The fundamental idea behind the SPI can be applied to

80   other hydrometeorological variables with the objective of building a standardized drought

81   index (Van Loon 2015; Kumar et al. 2016).

82   Each drought index has limitations and strengths in measuring drought conditions. For

83   instance, previous studies have shown that the SPI is more likely to detect the emergence of

84   drought conditions, whereas drought persistence can be more effectively identified based on

85   the SM deficit (Mo 2011). In other words, drought information based on a single index may

86   not be sufficient to provide an integrated picture of different types of drought (Kao &

87   Govindaraju 2010). This issue has, in turn, led to the need for a combination of multiple

88   drought indices that are derived from different hydrologic variables including rainfall, SM,

89   groundwater and streamflow. Such hydrological variables particularly have been used to

90   construct a joint drought index to characterize the complex nature of drought (Mirabbasi et al.

91   2012; Hao & Singh 2015).

92   Considering that drought is a multidimensional phenomenon, combining multiple variables

93   (e.g., from precipitation to SM) is beneficial for successful drought preparedness and

94   mitigation, and particularly useful for communication purposes between different types of

95   drought. Here, we adopt the MSDI proposed by Hao and AghaKouchak (2013) that can

96   combine meteorological and agricultural droughts, and the composite drought index was then

97   grouped by the hierarchical agglomerative clustering approach for classifying regional

98   patterns. Over the past decade, many researchers have proposed statistical models to build a

99   multivariate drought index. In the context of multivariate analysis, copulas have been used in

100   a wide range of hydrological studies such as multivariate drought frequency analysis (e.g.,

101   Ekanayake and Perera, 2014; Kao and Govindaraju, 2010; Kwon *et al.*, among others), flood

102   frequency/risk analysis (e.g., Favre *et al.*, 2004; Jongman *et al.*, 2014; Zhang and Singh,

103   2006), and rainfall simulation (Li et al. 2013). In this study, because of the interdependence

104   and interaction between rainfall and SM, the copula-based MSDI (Hao and AghaKouchak,

105   2013) is used to consider the two indices (i.e., the SPI and SSI) jointly in the context of a

106   multivariate probability distribution.

107   A key aim of this study is to explore a spatio-temporal drought pattern on the regional scale.

108   A number of previous studies have been carried out to investigate regional drought patterns

109   using cluster analysis, principal component analysis (PCA) or a combination of the two

110   techniques. Among them, clustering analysis, also known as an unsupervised classification

111   model, is widely used to classify drought patterns into certain categories according to their

112   relationships; such analysis can identify specific spatio-temporal patterns within the cluster

113   (Shamshirband et al. 2015). Santos et al. (2010) employed K-means clustering and PCA to

114   assess spatial and temporal patterns of the SPI series, whereas Yoo et al. (2012) applied the

115   K-means approach to partition their study region into several sub-regions based on bivariate

116   drought attributes. Furthermore, spatio-temporal drought patterns were regionally

117   summarized by combining a quantile regression model and hierarchical agglomerative

118   clustering algorithm (Shiau & Lin 2016; Yang et al. 2017). Despite the above-mentioned

119   potential uncertainty in identifying drought features using a drought index based on a single

120   variable, clustering analysis has not been applied extensively for a multivariate drought

121   index. In other words, most studies on clustering analysis were dedicated to the delineation of

122   homogeneous regions using a single drought index or their drought characteristics (e.g.,

123   duration, severity, and frequency).

124   Moreover, given that the nonstationarity in drought episodes is of increasing concern, the

125   nonparametric Mann-Kendall (MK) test has been widely used to identify significant changes

126   in drought pattern (Subash & Ram Mohan 2011; Güner Bacanli 2017). Despite its popularity

127   in the hydrological community, the MK approach cannot be applied to explore the temporal

128   variability of hydrologic variables at various quantiles of the distribution (Shiau & Lin 2016),

129   which is important for water resources management, especially for extreme rainfall that

130   translates into both droughts and floods. In this regard, this study uses a quantile regression

131   model proposed by Koenker and Bassett (1978) to explore the non-Gaussian distribution of

132   trend in drought characteristics in terms of the predefined quantiles (e.g., moderate, severe

133   and extreme drought).

134   The main contributions of this study are threefold: (1) we propose to use a global reanalysis

135   SM dataset to derive the SSI drought indices and its use to explore the transition from

136   meteorological to agricultural droughts; (2) we propose quantile regression model-based

137   spatio-temporal drought analysis at different quantiles, and (3) we classify spatio-temporal

138   drought patterns using the multivariate drought index and the hierarchical agglomerative

139   clustering approach, covering the period 1986-2016 across South Korea.

140   A brief background of this study was presented in this section. In the following section, we

141   illustrate the precipitation and SM data and further describe the drought indices considered in

142   this study. The theoretical aspects of modeling approaches including quantile regression,

143   copula function and clustering analysis are provided in Section 3. The spatio-temporal

144   analysis of the drought indices over South Korea obtained from this study is illustrated in

145   Section 4, followed by conclusions and future tasks in Section 5.

146

147   **2. Hydrologic Data and Drought Indices**

148   **2.1. Precipitation and Soil Moisture Data**

149   The historical daily precipitation data measured at 55 weather stations over South Korea,

150   which are operated by Korea Meteorological Administration (https://web.kma.go.kr/eng/), are

151   collected for the period 1986-2016. Figure 1 shows the locations of weather stations used in

152   this study. Additionally, a global SM data set from the European Centre for Medium-Range

153   Weather Forecasts (ECMWF) are used. ECMWF releases global reanalysis SM datasets (i.e.

154   ERA-Interim) daily in quasi-real time with high spatial resolution, in 6-hour intervals, at four

155   depths (i.e., 0-7, 7-28, 28-100 and 100-289 cm) (Albergel et al. 2012). ERA-Interim

156   reanalysis data provides a spatial resolution of approximately 25 km covering the period

157   1979-present and can be accessed from *https://www.ecmwf.int/*. The accuracy of the ERA-

158   Interim reanalysis data was assessed against in-situ observations from 117 stations across the

159   world by Albergel et al. (2012). Their results revealed robustness for various climate

160   conditions with a reasonable level of accuracy; similar results were also achieved based on

161   our preliminary analysis in the study area (see Figure S1). The Pearson correlation

162   coefficients between the original ERA-Interim and the currently available in-situ SM data

163   over all of South Korea are reasonably high, ranging from 0.60 to 0.75.

164   In our study, SM data are collected at 6-hour intervals (0:00, 6:00, 12:00 and 18:00 UTC)

165   from the locations with centroids nearest to the weather stations and averaged to obtain a

166   daily mean SM time series. The root-zone SM has a significant impact on crop yield so that it

167   is evident that crop growth and root development should take into consideration in designing

168   agricultural drought indices (Narasimhan & Srinivasan 2005). In this respect, the ERA-

169   Interim SM data at the third layer (28-100 cm) are mainly used as the best proxy of the root-

170   zone SM in this study. Both rainfall and SM data are then accumulated on a monthly basis for

171   subsequent study.

172   **[Fig. 1; Tab. 1]**

173

174   **2.2. SPI and SSI Drought Indices**

175   The SPI has been widely used to effectively measure and detect the extent of a deficit of

176   precipitation, providing locally specific early warnings of drought (Clayton 1978). Its

177   popularity stems from its flexibility and ease of use for detecting droughts at multiple time

178   scales (Ganguli & Ganguly 2016). Since the SPI was designed to provide a dimensionless

179   index, SPI values can often be used to spatio-temporally compare an overall view of the

180   drought at a national or global scale for a range of practical applications (Djerbouai & Souag-

181   Gamane 2016). To compute the SPI, daily precipitation data is first aggregated at different

182   timescales (e.g., 3, 6, 12, 24 or 36 months). In this study, we primarily focus on the SPI at 3-

183   and 6-month timescales (hereinafter, SPI-3/6) to investigate the characteristics of

184   meteorological droughts and their spatio-temporal patterns. The aggregated precipitation data

185   are typically fitted to theoretical distribution functions such as the gamma and Pearson type

186   III distributions (Farahmand & AghaKouchak 2015). The SPI is then computed by

187   transforming the cumulative probability distribution into standardized normal variates with

188   zero mean and standard deviation equal to one (Mckee et al. 1993; Guttman 1999). However,

189   because the optimal probability distribution of rainfall can vary substantially, a parametric

190   approach is less flexible, leading to inconsistent results (Vidal et al. 2009; Kumar et al. 2016;

191   Farahmand & AghaKouchak 2015). In other words, the SPI values are inherently susceptible

192   to the selection of a distribution function. Therefore, we employ a non-parametric kernel

193   density estimation approach to reduce the sampling error associated with the choice of

194   distribution functions. While the SPI is mainly used to identify meteorological drought,

195   agricultural drought is generally represented by the SM deficit. Accordingly, the SSI, known

196   as an agricultural drought index monitoring the extent and degree of SM, plays a

197   complementary role in a comprehensive review of drought conditions. Similarly, the kernel

198   density estimation approach was used to transform SM data into the SSI. In this study, we

199   extracted information on the durations and severities (i.e., deficit volumes) from SPI and SSI

200   time series. Drought duration refers to the periods of the continuously negative phase,

201   whereas drought severity is the sum of cumulative deficits over the corresponding duration

202   (Kwon et al., 2016). Table 2 shows the SPI drought criteria defined by Mckee et al. (1993).

203   Note that the same drought severity categories are subsequently applied to the SSI and MSDI.

204   **[Tab. 2]**

205

206   **3. Methodology**

207   **3.1. Quantile Regression**

208   This study aims to assess not only the overall trends of drought characteristics but also the

209   non-Gaussian distribution of trends in drought duration, severity and frequency at various

210   levels of quantiles. The first-order quantile regression (Koenker and Bassett, 1978) is applied

211   to identify temporal trends in different drought characteristics. The τth quantile regression

212   estimate is computed by minimizing Equation 1 as follows:

213    $$min\sum\nolimits_{i\,:\,y_i\,\geq\,\alpha_\tau+\beta_\tau x_i}\tau|y_i-\alpha_\tau-\beta_\tau x_i| + \sum\nolimits_{i:\,y_i\,<\,\alpha_\tau+\beta_\tau x_i}(1-\tau)|y_i-\alpha_\tau-\beta_\tau x_i| \qquad (1)$$

214   …where α_τ and β_τ are regression coefficients associated with the quantile τ, ranging between

215   0 and 1, and y indicates the drought indices (i.e., the SPI and SSI). In this study, the null

216   hypothesis of a zero slope for drought characteristics was tested at a level of 95% at quantile

217   τ.

218

219   **3.2. Overview of the Copula Function**

220   In order to better represent the interdependence between precipitation and SM, we used the

221   MSDI based on the joint distribution of two drought indices (i.e., the SPI and SSI). Among

222   various types of multivariate models, the copula has been widely applied in various areas

223   including hydrological and climatological applications since the copula can effectively link

224   the marginal distributions together to construct the joint distribution (Kwon et al. 2016; Kao

225   & Govindaraju 2010; Favre et al. 2004). From a modeling viewpoint, Sklar's Theorem (Sklar

226   1959) allows us to model the marginal distributions separately from the dependence structure,

227   which is described by a copula parameter C (Rüschendorf 2009; Lall et al. 2016; Requena et

228   al. 2013; Salvadori & De Michele 2004). The proposed approach provides a useful

229   framework to assess overall drought conditions since the MSDI can integrate different

230   aspects of drought dynamics, covering meteorological and agricultural droughts. Here, we

231   briefly introduce the concept of the copula. For more details, readers are kindly referred to

232   Joe (1997); Nelsen (1999); and Salvadori and De Michele (2004). Let the SPI and the SSI be

[9]

233   continuous random variables *X* and *Y*. If a joint distribution exists with the marginal

234   distribution $F(X)$ and $G(Y)$, then the cumulative joint probability p with a copula C can be

235   represented as Eq. (2):

236                    $P(X \leq x, Y \leq y) = C[F(X), G(Y)] = p$ (2)

237   Finally, the cumulative joint probability (p) of the SPI and SSI can be transformed into the

238   MSDI as follows (Hao & AghaKouchak 2013)…

239                    $MSDI = \varphi^-(p)$ (3)

240   …where φ^- is the inverse of the standard normal distribution function. The parameters of the

241   copula functions are estimated using the maximum likelihood (ML) method, and the optimal

242   copula for drought variables (i.e., *X* and *Y*) is then selected based on the Akaike Information

243   Criteria (AIC) (Akaike 1974). In this study, an optimal copula for each station is selected

244   from five copula functions (i.e., Gaussian, t, Clayton, Frank and Gumbel). More details are

245   found in Li et al., (2013) and Clayton, (2016).

246

247   **3.3. Clustering Analysis**

248   The hierarchical agglomerative clustering analysis is adopted to classify spatio-temporal

249   drought patterns into certain categories, which is carried out in the MATLAB environment.

250   The algorithm, application and implementation of this technique can be found in the literature

251   (Martinez & Martinez 2004). In this manner, weather stations are partitioned into subsets by

252   defining a measure of distance or dissimilarity in terms of drought features. In other words,

253   each category should be mutually exclusive, and the drought characteristics assigned to a

254   certain category should be as similar as possible. The hierarchical agglomerative clustering

255   approach begins with a measure of the similarity (or dissimilarity) between the objects (i.e.

256   the MSDI time series over 55 weather stations) that are initially regarded as an individual

257   cluster, and the individual clusters are then successively merged until one cluster includes all

258   objects. In this study, Ward's method, which is referred to as an increase of sum-of-squares,

259   is used to assess the proximity between two clusters…

260    $$(r, s) = \sqrt{\frac{2n_r n_s}{(n_r + n_s)}} \; ||\bar{x}_r - \bar{x}_s||_2 \qquad\qquad (4)$$

261   …where $|| \;||_2$ is the Euclidean distance, $\bar{x}_r$ and $\bar{x}_s$ are the centroids of clusters r and s, and n_r

262   and n_s are the number of elements in clusters r and s.

263

264   **4. Results and Discussion**

265   **4.1. Drought identification and Relationship between the SPI and SSI**

266   To explore drought propagation, we first evaluate cross-correlations between the SPI and SSI

267   to quantify the lag time over the entire array of weather stations for 3- and 6-month

268   accumulation periods, as shown in Figure 2 (Samples of cross-correlation between the SPI-n

269   and SSI-n can be seen in Figure 3). Here, the strongest cross-correlation at each station is

270   marked by a black dot. In other words, it appears to take one month at most weather stations

271   (i.e., 50 stations for 3-month and 48 stations for 6-month accumulation periods out of 55

272   weather stations, respectively) for precipitation deficits to propagate to SM deficits through

273   the hydrological cycle. In addition to the above drought features, an understanding of drought

274   persistence, which has an impact on water resources management, is also of great interest for

275   hydrologists (Meng et al. 2017; Ganguli & Ganguly 2016; AghaKouchak 2015). Drought

276   persistence can be computed by the length of a dry spell for a certain threshold or by using

277   temporal autocorrelations (Tatli 2015).

278   **[Figs. 2-3]**

279   We further explore a monthly variation of the correlation coefficient between the SPI-3 and

280   SSI-3 for the 55 weather stations, and the lagged relationships between the drought indices

281   are additionally examined to capture any possible delayed response. As shown in Figure 4,

282   the SPI is in general positively correlated with the SSI, thus confirming that the deficit of SM

[11]

283   is substantially related to the meteorological drought (Van Loon 2015). However, there exist

284   seasonal variations in correlation coefficients, which can be explained by the fact that

285   agricultural drought in response to the deficit in rainfall may differ significantly, depending

286   on the season. Furthermore, it can be concluded that the stronger relationship begins when

287   rainfall starts after a long, dry winter-spring season in South Korea. In this stage, the water

288   moves both through the soil and over the surface via a range of hydrologic processes such as

289   base flow, seepage, infiltration and runoff throughout the summer. In contrast, the

290   relationship weakens as SM content decreases below the wilting point, with the relationship

291   continuing to weaken until the next wet season. Interestingly, it appears that during a dry

292   season (winter-spring), there is a more robust relationship between the SPI and the 1-month

293   lagged SSI. It can be concluded that the SSI has a delayed response to the SPI under dry soil

294   conditions, whereas for wet soil conditions, the prompt response of the SSI to the SPI is

295   dominant. In this perspective, it is acknowledged that the characteristics of the transition from

296   meteorological drought to agricultural drought are significantly dependent on antecedent SM

297   content over the season. Thus, we should consider the issue of presenting the role of

298   antecedent SM content in connection with evidence concerning changes in the drought

299   propagation feature over time.

300   **[Fig. 4]**

301   We investigate the temporal persistence of the drought indices using the autocorrelation

302   function representing drought persistence over the entire array of weather stations. As shown

303   in Figure 5, it is evident that the autocorrelation functions of SSI decrease gradually with

304   higher degrees of autocorrelation compared to that of the SPI for both accumulation periods.

305   On the other hand, the results also highlight the potential benefit of using different drought

306   indices, i.e., the onset of a drought condition can be detected by the meteorological index

307   (i.e., the SPI) earlier, whereas the SSI seems to be more appropriate for reliably describing

308   drought persistence (Farahmand & AghaKouchak 2015; Entekhabi et al. 1996). In this

309   regard, we introduced a robust framework that allows multiple drought indices to be

310   combined. The results associated with the combined drought indices are presented in Section

311   4.3.

312   **[Fig. 5]**

313

314   **4.2. Spatial Pattern of Drought over South Korea**

315   For each accumulation period (3- and 6- month), drought events are identified using a

316   threshold of -1.0 and their spatial distributions along with durations are displayed in Figure 6.

317   The cokriging method (Pebesma 2004) is hereinafter employed to obtain the regional

318   distribution of drought characteristics. Compared to the SPI, the SSI shows less frequent

319   droughts for both accumulation periods, which can be attributed to the stronger persistence

320   (i.e., a smaller fluctuation) that is more likely to be characterized by the SSI (Farahmand &

321   AghaKouchak 2015). Furthermore, more frequent drought events appear to occur at a shorter

322   timescale for both drought indices (Figures 6c and g), due to the relatively weaker persistence

323   (Figures 6d and h). It was also clearly seen that drought duration of the SSI is significantly

324   longer than that of the SPI, and the difference becomes more distinct for a longer timescale.

325   In other words, the 3-month drought indices pertain negative values more frequently than do

326   the 6-month drought indices, and the SPI recovers to wet states more quickly than does the

327   SSI. More frequent drought events with the threshold -1.0 particularly stand out in western

328   central South Korea for the SPI, while an increased frequency of moderate droughts is

329   identified in the southern and northern parts of South Korea.

330   **[Fig. 6]**

331   Next, drought characteristics such as duration and severity for the SPI and SSI are extracted

332   and their spatial distributions are presented in Figures 7 and 8. For SPI-3, a longer drought

333 duration is predominantly identified in the northern and southern parts of South Korea and

334 the magnitude of drought severity is found to be similar to the spatial distribution of drought

335 duration. Yet, as the accumulation period increases (i.e., SPI-6), the spatial extent of droughts

336 is partially extended to the east coast. As expected, for both drought accumulation periods,

337 the spatial distribution of drought over South Korea clearly reveals the strong spatial

338 coherence between drought duration and severity. That is, regions with a prolonged drought

339 tend to experience more severe droughts, leading to more severe effects on water resource

340 management and vice versa. Additionally, there is a tendency for duration and severity to

341 increase in proportion to the accumulation period for either SPI or SSI. As shown in Figures

342 7-8, there are some differences in the spatial distribution of duration and severity between the

343 SSI and SPI. It can be seen that the SSI consistently yields higher drought durations and

344 severities, compared with the SPI. Again, this may be attributed to the stronger persistence of

345 the SSI. Locally significant severe droughts in terms of both drought duration and severity

346 are primarily represented in the southeastern region. Interestingly, the spatial distribution of

347 drought characteristics associated with the SPI is more dependent on the accumulation

348 periods (see Figure 7), while the SSI is less sensitive to the accumulation periods (see Figure

349 8).

350   **[Figs. 7-8]**

351 The entire time series of the SPI-6 and SSI-6 were divided into two halves (i.e. 1st period

352 (1987-2001) and 2nd period (2002-2016)), and the drought events and their durations and

353 severities were extracted using a threshold of -1.5. Note that the values given here are the

354 average values over the entire weather stations during that period. For the SPI-6 (Figures 9a-

355 c), the number of drought events are significantly decreased in the second half, while the

356 duration and severity are slightly increased. It can be concluded that the decreasing trend in

357 the drought events is apparently due to an increasing trend in precipitation since the SPI

358   represents deficits in precipitation. Relative to the decreasing trend in the number of drought

359   events, a severe and prolonged drought has been observed over the last decade due to a recent

360   increase in interannual climate variability (Nam et al. 2015). On the other hand, for the SSI-6

361   (Figures 9d-f), a drought with more pronounced frequency and severity compared to the SPI-

362   6 was found in the second half. It may be the consequence of a significant increasing trend in

363   temperature during the recent period while the recent decrease in precipitation may play a

364   limited role for the tendency toward increased drought frequency and severity.

365   **[Fig. 9]**

366   The trends in the SPI and SSI time series covering 1986-2016 are further analyzed using a

367   quantile regression model. The estimated slope parameters for the predefined drought

368   categories (Table 2) at 55 weather stations are spatially interpolated. As shown in Figures 10a

369   and d, for both indices, the trends for moderate drought (i.e., threshold -1.0) showed a

370   downward tendency in the northern part of South Korea, while an upward trend is dominantly

371   localized in the southern region. Interestingly, there exist significant differences in the spatial

372   presence of trends in extreme drought (i.e., threshold -2.0) between the SPI and SSI. More

373   specifically, the SSI shows a decreasing tendency over the entire region, while there is no

374   significant difference in the spatial distribution of drought trend over different drought states

375   for the SPI. In summary, there appears to be a more pronounced decreasing tendency (or

376   increasing risk) of the drought in the northern part of South Korea. In South Korea, nearly 50-

377   60% of total annual rainfall occurs during the summer monsoon season (Kim et al. 2002). It

378   has been reported that a general declining trend is evident in the East Asian summer

379   monsoon, and this tendency appears to be more prevalent since the early 1990s (Li et al.

380   2017). Similarly, the increased drought risk in the northern part of South Korea may be

381   linked to weakened summer monsoons over the last three decades, which can be associated

382   with stagnation of the monsoon activity in the middle of South Korea, and then retreat toward

383   a lower latitude (Zhang & Zhou 2015).

384   **[Fig. 10]**

385

386   **4.3. Clustering Analysis on Multivariate Standardized Drought Index (MSDI)**

387   A hierarchical clustering approach is applied to explore regional trends in droughts over the

388   last three decades. One may consider a direct use of two drought indices for clustering

389   regional patterns. However, based on our preliminary analysis (see Figures S3-S4), the

390   distribution of the identified clusters in the SPI and SSI are significantly different, thus

391   confirming that the direct use of indices together for the clustering may fail to identify

392   regional patterns of drought. On the other hand, with multi-dimensional data, one can employ

393   multivariate techniques, such as copulas, which can provide a better estimation for

394   dependencies among the variables, prior to clustering. Specifically, we introduce the MSDI to

395   provide a comprehensive perspective of the drought by constructing a joint probability

396   distribution between the SPI and SSI. We consider two types of elliptical copulas and three

397   types of Archimedean copulas to model the dependency structure of the drought indices,

398   namely the student t, Gaussian, Clayton, Frank and Gumbel. As discussed in the

399   methodology section, the marginal distributions are first specified with the independent

400   identically distributed (IID) assumption for the drought variables, and the interdependence

401   between the variables is then described through the copula functions. In this study, it might

402   be desirable to assume the Gaussian distribution for the marginal distributions for both the

403   SSI and SPI, since the indices are already normalized to their respective values. A set of

404   parameters for the MSDI, four parameters in the marginal distribution and one parameter in

405   the copula function, are estimated by using the maximum likelihood method (Kao &

406   Govindaraju 2010; Renard & Lang 2007; Bouyé et al. 2000), and the optimal copula

407   functions are then selected using the Akaike Information Criteria (AIC) for each weather

408   station. Among five types of copulas, the Frank copula is generally selected for both

409   accumulation periods, and the spatial distribution of the selected copula is presented in Figure

410   S5.

411   We use clustering analysis to explore the presence of a regional trend in drought, and an

412   important issue with respect to the clustering approach is to determine the number of desired

413   clusters. To systematically choose the optimum number of clusters with the hierarchical

414   agglomerative clustering algorithm, the algorithm is recursively applied to the MSDI series

415   with an increasing number of clusters and the optimum number of clusters is selected by

416   maximizing (or minimizing) some measure of fitness. This study uses the upper-tail rule,

417   proposed by Mojena (1977), as a measure of model fitness. The best cut-off level (i.e., the

418   number of clusters) is determined by the distance analysis of the standardized fusion levels in

419   a dendrogram. As shown in Figure 11, the inflection points of the MSDI-3 is found at a cut-

420   off level of four (Figure 11a). In other words, the degree of decrease in the standardized

421   fusion level is negligible for more than four clusters. On the other hand, an inflection point is

422   found at five clusters for the MSDI-6 (Figure 11b). Therefore, four clusters for the MSDI-3

423   and five clusters for the MSDI-6 are subsequently selected for further analyses.

424   **[Fig. 11]**

425   The distribution of the resulting clusters is contiguous rather than spatially separated for both

426   accumulation periods, as presented in Figure 12. It can be concluded that the results are more

427   physically interpretable, which can lead to more effective strategies in the development and

428   implementation of drought management and mitigation plans for certain areas. There is a

429   notable contrast to the clustering over accumulation periods in the northern part of South

430   Korea, namely Gyeonggi province and Gangwon province. More specifically, two

431   subcategories, representing Gyeonggi and Gangwon province, in MSDI-6 are grouped

432   together as a category in MSDI-3. For a given cluster, this study further explores different

433   aspects of drought features such as duration, severity and long-term trends at different

434   quantile levels.

435   **[Fig. 12]**

436   The spatially averaged MSDI values over each cluster are shown in Figures 12-13, and their

437   trends appear to differ significantly between thresholds (or exceedance probabilities;

438   moderate (-1.0): 0.16, severe (-1.5): 0.07 and extreme (-2.0): 0.02). Compared to the MSDI-6,

439   more frequent drought events appear to be identified at the MSDI-3, and the number of

440   drought events for certain drought categories varies over different clusters, as summarized in

441   Table 3. It is evident that drought duration of the MSDI-6 is significantly longer than that of

442   the MSDI-3, and the difference becomes more distinct under extreme drought conditions.

443   Similarly, an overall increase in drought severity in the MSDI-6 is clearly observed.

444   Specifically, more moderate to severe drought episodes are observed in the northern part of

445   South Korea, covered by clusters CL-3 and CL-4 for the MSDI-3 and by clusters CL-1 and

446   CL-2 for the MSDI-6. Clusters CL-2 for the MSDI-3 and CL-4 for the MSDI-6 notably for

447   the longer duration period and the higher severity are mainly identified along the southern

448   coast, under moderate to severe drought condition. Spatially aggregated drought features vary

449   under extreme drought conditions. In other words, CL-3 for the MSDI-3 indicates a much

450   more extreme drought condition in the northern part of South Korea, and as does CL-4 for the

451   MSDI-6 in the southern coast.

452   **[Tab. 3]**

453   Additionally, we explore regional trends over predefined thresholds using a quantile

454   regression model, as represented in Figures 13-14 and Table 4. Numbers in bold are

455   statistically significant at the 0.05 level ($p < 0.05$) in Table 4. For the MSDI-3, CL-1

456   representing drought in the central eastern region showed no trend for all four levels, while a

457   significantly decreasing trend is shown in CL-3. A significantly decreasing trend (or

458   increasing drought risk) in MSDI-3 was found at CL-2 (e.g., median) and CL-4 (e.g.,

459   extreme, moderate and median). Overall, for a longer-duration MSDI-6, a significant

460   downward trend becomes more dominant. Furthermore, we explore the past three major

461   drought episodes over the last three decades (1986-2016), as illustrated in Figures 13-14. As

462   presented, drought episodes Ep1 (1994-1996), Ep2 (2000-2002) and Ep3 (2013-2015) are

463   clearly identified as major drought events that have been reported in previous studies (Min et

464   al. 2003; Kwon et al. 2016; Nam et al. 2015). As for Ep3, the amount of rainfall for this

465   period was less than 35-50% of the annual mean rainfall (1973-2015) and the estimated

466   return period was about 26 years (Kwon et al. 2016). Local governments during this dry

467   period implemented a plan to restrict water usage in many cities across South Korea, thus

468   confirming that the MSDI can accurately reproduce the historical drought.

469   **[Figs. 13-14; Tab. 4]**

470

471   **5. Concluding remarks**

472   Drought is an increasingly important issue in many parts of the world, requiring a hydro-

473   meteorological modeling framework to assess and monitor its complex impact on natural

474   hazards and associated socio-economic vulnerability. Here, we use two representative

475   drought indices (the SPI and SSI) to evaluate changes in drought patterns at different spatio-

476   temporal scales. The SPI and SSI, derived from precipitation and SM, respectively, are

477   compared with each other by describing their individual characteristics as drought indicators

478   as well as their interdependence and interaction. Furthermore, considering different aspects of

479   the drought dynamics, this study introduces the MSDI, which is used to consider

480   meteorological and agricultural droughts jointly in the context of a multivariate probability

481   distribution. The MSDI derived for each station is then grouped using the hierarchical

482   clustering approach for better understanding of the regional features of drought conditions.

483   The primary conclusions obtained in this study are as follows:

484   1. The transition from meteorological to agricultural drought is clearly identified, but the

485   degree of their relationship is significantly dependent on the season. Specifically, the

486   SSI had a 1-month delayed response to the SPI during the dry season (i.e., winter-

487   spring), whereas the response of the SSI to SPI is generally prompt under wet soil

488   conditions. Thus, one should consider the role of antecedent SM content to improve

489   characterization of changes in drought propagation.

490   2. The SSI shows less frequent droughts and longer drought duration, due to the gradual

491   decrease in the autocorrelation functions of SSI along with the higher degree of

492   autocorrelation, compared to that of the SPI. In this perspective, the onset of a drought

493   could be detected by the SPI, whereas the SSI appears to be more appropriate for

494   describing drought persistence. Overall, this is also supported by the fact that the 1-

495   month lag between the SPI and SSI was significant for most stations over the last

496   three decades (1986-2016).

497   3. In this study, the copula-based MSDI is employed to consider the interdependence

498   and interaction between rainfall and SM in the context of a multivariate probability

499   distribution. Moreover, the hierarchical agglomerative clustering approach is

500   employed to identify the spatial pattern of the MSDI. The distribution of the resulting

501   clusters is contiguous rather than spatially isolated for both accumulation periods,

502   contributing to more effective strategies in the development and implementation of

503   drought management and mitigation plans for certain areas.

504   4. Here, we use a hierarchical clustering approach to the MSDI to investigate regional

505   trends in drought pattern. By using this approach, the spatio-temporal drought patterns

506   are clearly captured through the MSDI. Specifically, more drought episodes under

507   moderate to severe drought conditions are dominantly observed along the southern

508   coast of South Korea. We also find persistent drought with a higher level of severity

509   in the northern part of South Korea, which might be attributable to the significant

510   decreasing trend (or increasing drought risk) that is noted in the northern part of South

511   Korea. Overall, for a longer-duration MSDI-6, a significant downward trend has

512   become more dominant.

513 Given that a drought index more effectively provides the status of drought for decision

514 making in near-real time compared to raw data, and that a single drought index may not be

515 sufficient for describing the complex aspects of drought, the findings and approaches used in

516 this study are expected to provide useful guidelines for detecting the nature of droughts and

517 contributing to drought preparedness. However, integration with other relevant drought

518 indicators (e.g., streamflow and ground water) is still needed for a better understanding of

519 multi-dimensional aspects of drought in future studies. Moreover, future work will also focus

520 on the extension of data records with multiple sources such as satellite remote sensing data

521 and multiple hydro-meteorological variables as potential predictors.

522

528

529 **References**

530 Agha Kouchak, A. 2015. A multivariate approach for persistence-based drought prediction:

531   Application to the 2010-2011 East Africa drought. *Journal of Hydrology*, **526**: 127-

532   135. doi: 10.1016/j.jhydrol.2014.09.063

533 Akaike, H. 1974. A New Look at the Statistical Model Identification. *IEEE Transactions on*
534   *Automatic Control*, **19(6)**: 716-723.

535 Albergel, C. et al. 2012. Soil Moisture Analyses at ECMWF: Evaluation Using Global
536   Ground-Based In Situ Observations. *Journal of Hydrometeorology*, **13(5)**: pp.1442-
537   1460. *http://journals.ametsoc.org/doi/abs/10.1175/JHM-D-11-0107.1*

538 Bouyé, E. et al. 2000. Copulas for Finance - A Reading Guide and Some Applications. *SSRN*
539   *Electronic Journal*. *http://www.ssrn.com/abstract=1032533*

540 Clayton, D. G. 1978. A Model for Association in Bivariate Life Tables and Its Application in
541   Epidemiological Studies of Familial Tendency in Chronic Disease Incidence.
542   *Biometrika*, **65(1)**: 141-151.

543 Dai, A. 2011. Drought under global warming: A review. *Wiley Interdisciplinary Reviews:*
544   *Climate Change*, **2(1)**: 45-65.

545 Djerbouai, S. & Souag-Gamane, D. 2016. Drought Forecasting Using Neural Networks,
546   Wavelet Neural Networks, and Stochastic Models: Case of the Algerois Basin in
547   North Algeria. *Water Resources Management*, **30(7)**: 2445-2464.

548 Dracup, J. A., Lee, K. S. & Paulson, E. G., 1980. On the definition of droughts. *Water*
549   *Resources Research*, **16(2)**: 297-302.

550 Ekanayake, E. & Perera, K. 2014. Analysis of Drought Severity and Duration Using Copulas
551   in Anuradhapura, Sri Lanka. *British Journal of Environment and Climate Change*,
552   **4(3)**: 312-327.
553   *http://www.sciencedomain.org/abstract.php?iid=631&id=10&aid=6867*

554 Entekhabi, D., Rodriguez-Iturbe, I. & Castelli, F., 1996. Mutual interaction of soil moisture
555   state and atmospheric processes. *Journal of Hydrology*, **184(1-2)**: 3-17.

556 Farahmand, A. & Agha Kouchak, A. 2015. A generalized framework for deriving
557   nonparametric standardized drought indicators. *Advances in Water Resources*, **76**:
558   140-145. doi: 10.1016/j.advwatres.2014.11.012

559 Favre, A. C. et al. 2004. Multivariate hydrological frequency analysis using copulas. *Water*
560   *Resources Research*, **40(1)**: 1-12.

561 Ganguli, P. & Ganguly, A. R. 2016. Space-time trends in U.S. meteorological droughts.
562   *Journal of Hydrology: Regional Studies*, **8**: 235-259. doi: 10.1016/j.ejrh.2016.09.004

563 Güner Bacanli, Ü. 2017. Trend analysis of precipitation and drought in the Aegean region,
564   Turkey. *Meteorological Applications*, **24(2)**: 239-249.

565   Guttman, N. B. 1999. Accepting the Standardized Precipitation Index: a Calculation
566   Algorithm1. *JAWRA Journal of the American Water Resources Association*, **35(2)**:
567   311-322.

568   Hao, Z. & AghaKouchak, A. 2013. Multivariate Standardized Drought Index: A parametric
569   multi-index model. *Advances in Water Resources*, **57**: 12-18. doi:
570   10.1016/j.advwatres.2013.03.009

571   Hao, Z. & Singh, V. P. 2015. Drought characterization from a multivariate perspective: A
572   review. *Journal of Hydrology*, **527**: 6680678. doi: 10.1016/j.jhydrol.2015.05.031

573   Hayes, M. et al. 2011. The lincoln declaration on drought indices: Universal meteorological
574   drought index recommended. *Bulletin of the American Meteorological Society*, **92(4)**:
575   485-488.

576   Joe, H., 1997. *NoMultivariate Models and Multivariate Dependence Concepts*, New York:
577   Chapman and Hall.

578   Jongman, B. et al. 2014. Increasing stress on disaster-risk finance due to large floods. *Nature*
579   *Climate Change*, **4(4)**: 264-268.

580   Kao, S. C. & Govindaraju, R. S., 2010. A copula-based joint deficit index for droughts.
581   *Journal of Hydrology*, 380(1-2): 121-134. doi: 10.1016/j.jhydrol.2009.10.029

582   Kim, B. J. et al. 2002. Summer monsoon rainfall patterns over South Korea and associated
583   circulation features. *Theoretical and Applied Climatology*, **72(1-2)**: 65-74.

584   Koenker, R. & Bassett, G. 1978. Regression quantiles. *Econometrica*, **46(1)**: 33-50.

585   Kumar, R. et al. 2016. Multiscale evaluation of the Standardized Precipitation Index as a
586   groundwater drought indicator. *Hydrology and Earth System Sciences*, **20(3)**: 1117-
587   1131.

588   Kwon, H. H., Lall, U. & Kim, S. J. 2016. The unusual 2013-2015 drought in South Korea in
589   the context of a multicentury precipitation record: Inferences from a nonstationary,
590   multivariate, Bayesian copula model. *Geophysical Research Letters*, **43(16):** 8534-
591   8544.

592   Lall, U., Devineni, N. & Kaheil, Y. 2016. An Empirical, Nonparametric Simulator for
593   Multivariate Random Variables with Differing Marginal Densities and Nonlinear
594   Dependence with Hydroclimatic Applications. *Risk Analysis*, **36(1)**: 57-73.

595   Li, C., Singh, V. P. & Mishra, A. K. 2013. A bivariate mixed distribution with a heavy-tailed
596   component and its application to single-site daily rainfall simulation. *Water Resources*
597   *Research*, **49(2)**: 767-789.

598   Li, X. et al. 2017. The East Asian summer monsoon variability over the last 145 years
599   inferred from the Shihua Cave record, North China. *Scientific Reports*, **7(1)**: 1-11. doi:
600   10.1038/s41598-017-07251-3

601   van Loon, A. F. et al. 2016. Drought in a human-modified world: Reframing drought
602   definitions, understanding, and analysis approaches. *Hydrology and Earth System*
603   *Sciences*, **20(9)**: 3631-3650.

604   van Loon, A. F. 2015. Hydrological drought explained. *Wiley Interdisciplinary Reviews:*
605   *Water*, **2(4)**: 359-392. doi: 10.1002/wat2.1085

606   Martinez, W. L. & Martinez, A. R. 2004. *Exploratory Data Analysis with MATLAB*. doi:
607   10.1201/9780203483374

608   Mckee, T. B., Doesken, N. J. & Kleist, J. 1993. The relationship of drought frequency and
609   duration to time scales. *AMS 8th Conference on Applied Climatology*, (January), 179-
610   184. *http://ccc.atmos.colostate.edu/relationshipofdroughtfrequency.pdf*

611   Meng, L., Ford, T. & Guo, Y. 2017. Logistic regression analysis of drought persistence in
612   East China. *International Journal of Climatology*, **37(3)**: 1444-1455.

613   Min, S. K. et al. 2003. Spatial and temporal comparisons of droughts over Korea with East
614   Asia. *International Journal of Climatology*, **23(2)**: 223-233.

615   Mirabbasi, R. et al. 2013. Analysis of meteorological drought in northwest Iran using the
616   Joint Deficit Index. *Journal of Hydrology*, **492**: 35-48. doi:
617   10.1016/j.jhydrol.2013.04.019

618   Mirabbasi, R., Fakheri-Fard, A. & Dinpashoh, Y. 2012. Bivariate drought frequency analysis
619   using the copula method. *Theoretical and Applied Climatology*, **108(1-2)**: 191-206.

620   Mo, K. C. 2011. Drought onset and recovery over the United States. *Journal of Geophysical*
621   *Research Atmospheres*, **116(20)**: 1-14.

622   Mojena, R., 1977. Hierarchical grouping methods and stopping rules: An evaluation. *Coputer*
623   *Journal*, 20 (April), 359-363.

624   Nam, W. H. et al. 2015. Drought hazard assessment in the context of climate change for
625   South Korea. *Agricultural Water Management*, **160**: 106-117. doi:
626   10.1016/j.agwat.2015.06.029

627   Narasimhan, B. & Srinivasan, R. 2005. Development and evaluation of Soil Moisture Deficit
628   Index (SMDI) and Evapotranspiration Deficit Index (ETDI) for agricultural drought
629   monitoring. *Agricultural and Forest Meteorology*, **133(1-4)**: 69-88.

630   Nelsen, R. B. 1999. An Introduction to Copulas. In New York: Springer.

631   Palmer, W. C. 1965. Meteorological Drought. *U.S. Weather Bureau, Res. Pap. No. 45*, 58.
632   *https://www.ncdc.noaa.gov/temp-and-precip/drought/docs/palmer.pdf*

633   Pebesma, E. J., 2004. Multivariable geostatistics in S: The gstat package. *Computers and*
634   *Geosciences*, **30(7)**: 683-691.

635   Renard, B. & Lang, M. 2007. Use of a Gaussian copula for multivariate extreme value
636   analysis: Some case studies in hydrology. *Advances in Water Resources*, **30(4)**: 897-
637   912.

638   Requena, A. I., Mediero, L. & Garrote, L. 2013. A bivariate return period based on copulas
639   for hydrologic dam design: Accounting for reservoir routing in risk estimation.
640   *Hydrology and Earth System Sciences*, **17(8)**: 3023-3038.

641   Rüschendorf, L. 2009. On the distributional transform, Sklar's theorem, and the empirical
642   copula process. *Journal of Statistical Planning and Inference*, **139(11)**: 3921-3927.

643   Salvadori, G. & de Michele, C. 2004. Frequency analysis via copulas: Theoretical aspects and
644   applications to hydrological events. *Water Resources Research*, **40(12)**: 1-17.

645   Santos, J. F., Pulido-Calvo, I. & Portela, M. M. 2010. Spatial and temporal variability of
646   droughts in Portugal. *Water Resources Research*, **46(3)**: 1-13.

647   Shafer, B. A. & Dezman, L. E., 1982. Development of a surface water supply index (SWSI)
648   to assess the severity of drought conditions in snowpack runoff areas. *Western Snow*
649   *Conference*, 164-175.

650   Shamshirband, S. et al. 2015. Clustering project management for drought regions
651   determination: A case study in Serbia. *Agricultural and Forest Meteorology*, **200**: 57-
652   65.

653   Shiau, J. T. & Lin, J. W., 2016. Clustering Quantile Regression-Based Drought Trends in
654   Taiwan. *Water Resources Management*, **30(3)**: 1053-1069.

655   Shukla, S., Steinemann, A. C. & Lettenmaier, D. P. 2011. Drought Monitoring for
656   Washington State: Indicators and Applications. *Journal of Hydrometeorology*, **12(1)**:
657   66-83. doi: 10.1175/2010JHM1307.1

658   Sklar, M., 1959. Fonctions de Répartition À N Dimensions Et Leurs Marges. In Publications
659   de l'Institut de Statistique de L'Université de Paris 8, 229-231.

660   Spinoni, J. et al. 2014. World drought frequency, duration, and severity for 1951-2010.
661   *International Journal of Climatology*, **34(8)**: 2792-2804.

662   Sprenger, M. et al., 2016. A copula-based nonstationary frequency analysis for the 2012-2015
663   drought in California. *Water Resources Research*, **52**: 5727-5754.

664 Subash, N. & Ram Mohan, H. S. 2011. Trend detection in rainfall and evaluation of
665   standardized precipitation index as a drought assessment index for rice-wheat
666   productivity over IGR in India. *International Journal of Climatology*, 31(11), 1694-
667   1709.

668 Svoboda, M. D. & Fuchs, B. A. 2017. *Handbook of drought indicators and indices*.

669 Tatli, H. 2015. Detecting persistence of meteorological drought via the Hurst exponent.
670   *Meteorological Applications*, **22(4)**: 763-769.

671 Vicente-Serrano, S. M., Beguería, S. & López-Moreno, J. I. 2010. A multiscalar drought
672   index sensitive to global warming: The standardized precipitation evapotranspiration
673   index. *Journal of Climate*, **23(7)**: 1696-1718.

674 Vidal, J.-P. et al. 2009. Multilevel and multiscale drought reanalysis over France with the
675   Safran-Isba-Modcou hydrometeorological suite. *Hydrology and Earth System
676   Sciences Discussions*, **6(5)**: 6455-6501. *http://www.hydrol-earth-syst-sci-
677   discuss.net/6/6455/2009/*

678 Yang, P. et al. 2017. Quantile regression and clustering analysis of standardized precipitation
679   index in the Tarim River Basin, Xinjiang, China. *Theoretical and Applied
680   Climatology*.

681 Yoo, J. et al. 2012. Drought frequency analysis using cluster analysis and bivariate
682   probability distribution. *Journal of Hydrology*, **420-421**: 102-111. doi:
683   10.1016/j.jhydrol.2011.11.046

684 Zargar, A. et al., 2011. A review of drought indices. *Environmental Reviews*, **19(NA)**: 333-
685   349. doi: /10.1139/a11-013

686 Zhang, L. & Singh, V. P. 2006. Bivariate Flood Frequency Analysis Using the Copula
687   Method. *Water*, 11 (April): 150-164.

688 Zhang, L. & Zhou, T., 2015. Drought over East Asia: A review. *Journal of Climate*, 28(8):
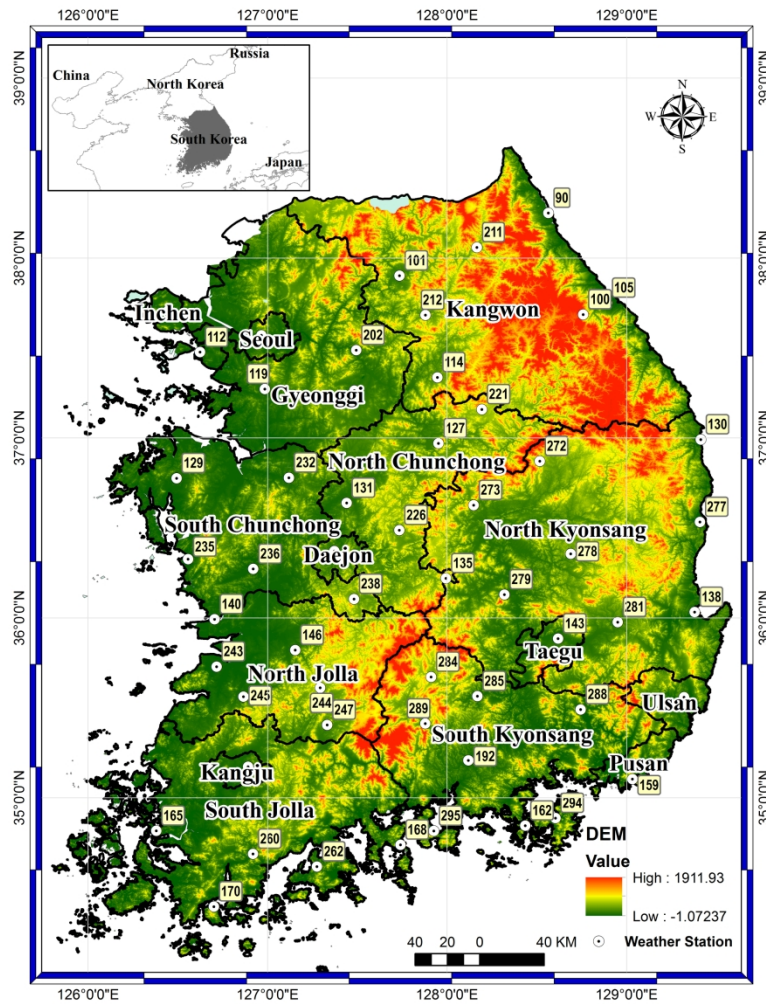689   3375-3399.

Figure 1. Topographic map showing the locations of weather stations used in this study. Here, black solid lines indicate province boundaries.
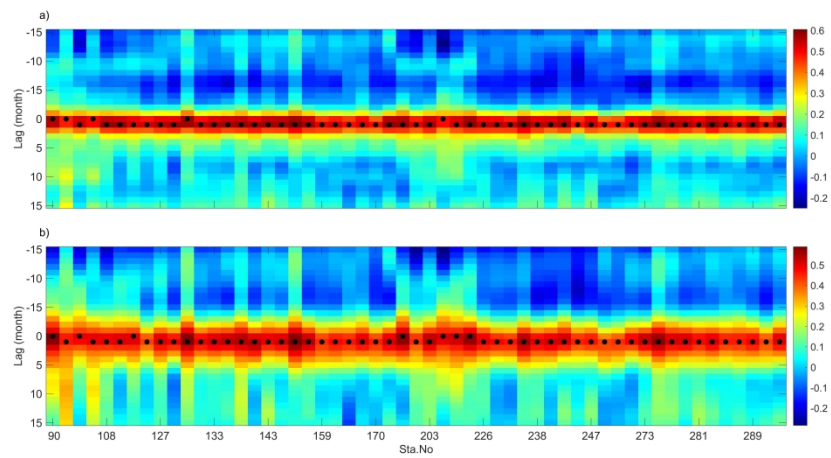
210x296mm (300 x 300 DPI)

Figure 2. Heat maps showing cross-correlation coefficients between SPI and lagged SSI over the entire array of weather stations. Here, a) and b) represent accumulation periods of 3 and 6 months, respectively.
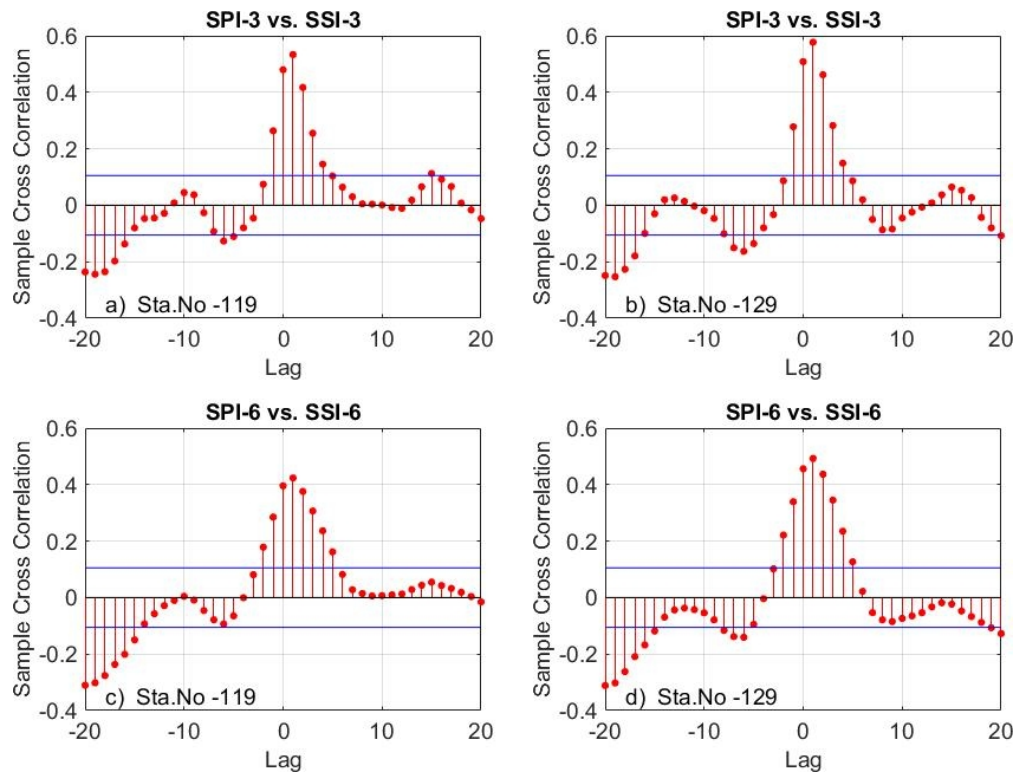
508x266mm (300 x 300 DPI)

Figure 3. Samples of cross-correlation between SPI and SSI for 3- and 6-month time scale.
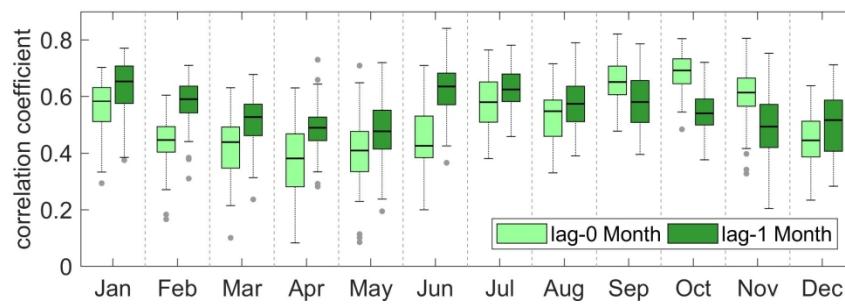
71x54mm (300 x 300 DPI)

Figure 4. Boxplots of the Pearson correlation coefficients for identifying time-lagged relationships between the SPI-3 and SSI-3 time series on a monthly basis across all stations.
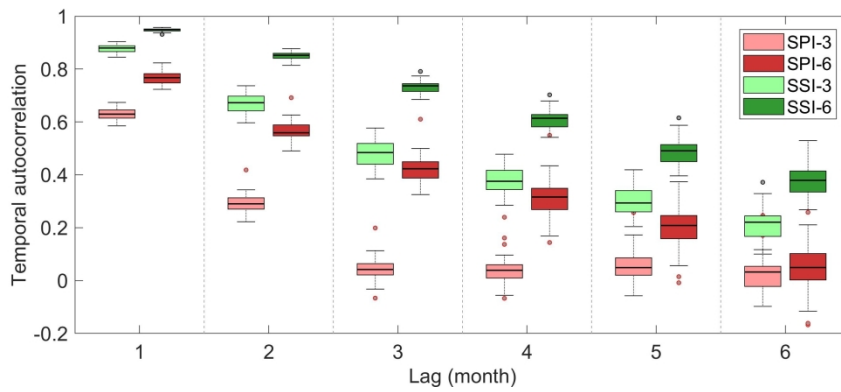
211x66mm (300 x 300 DPI)

Figure 5. Temporal autocorrelation functions of SPIs and SSIs representing drought persistence with respect to different time lags.
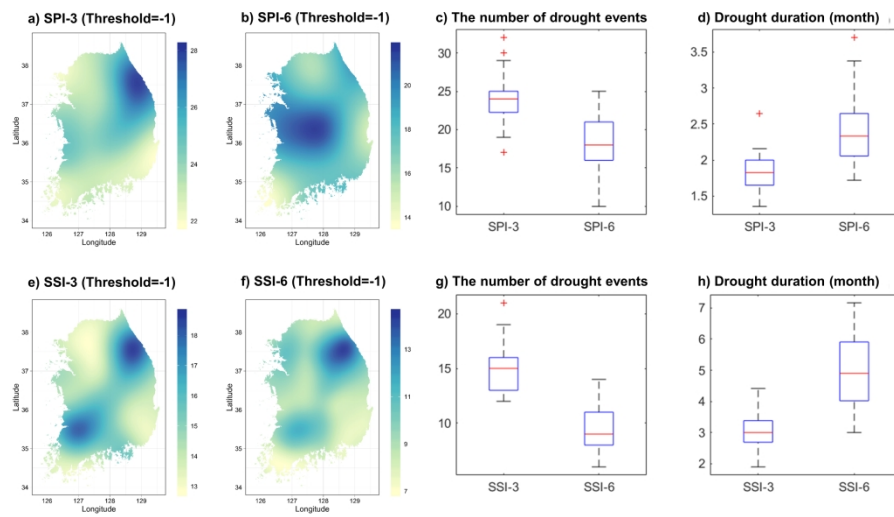
264x105mm (300 x 300 DPI)

Figure 6. Characteristics of SPI/SSI-n drought events based on a threshold of -1.0 (moderate drought): a-b and e-f show the spatial distributions of drought events across South Korea along with their boxplots (c and g), and their corresponding average drought durations are presented in d and h.

338x190mm (300 x 300 DPI)

Figure 7. Spatial distribution patterns of meteorological drought (SPI-n) duration and severity using a threshold of -1.0 (moderate drought).
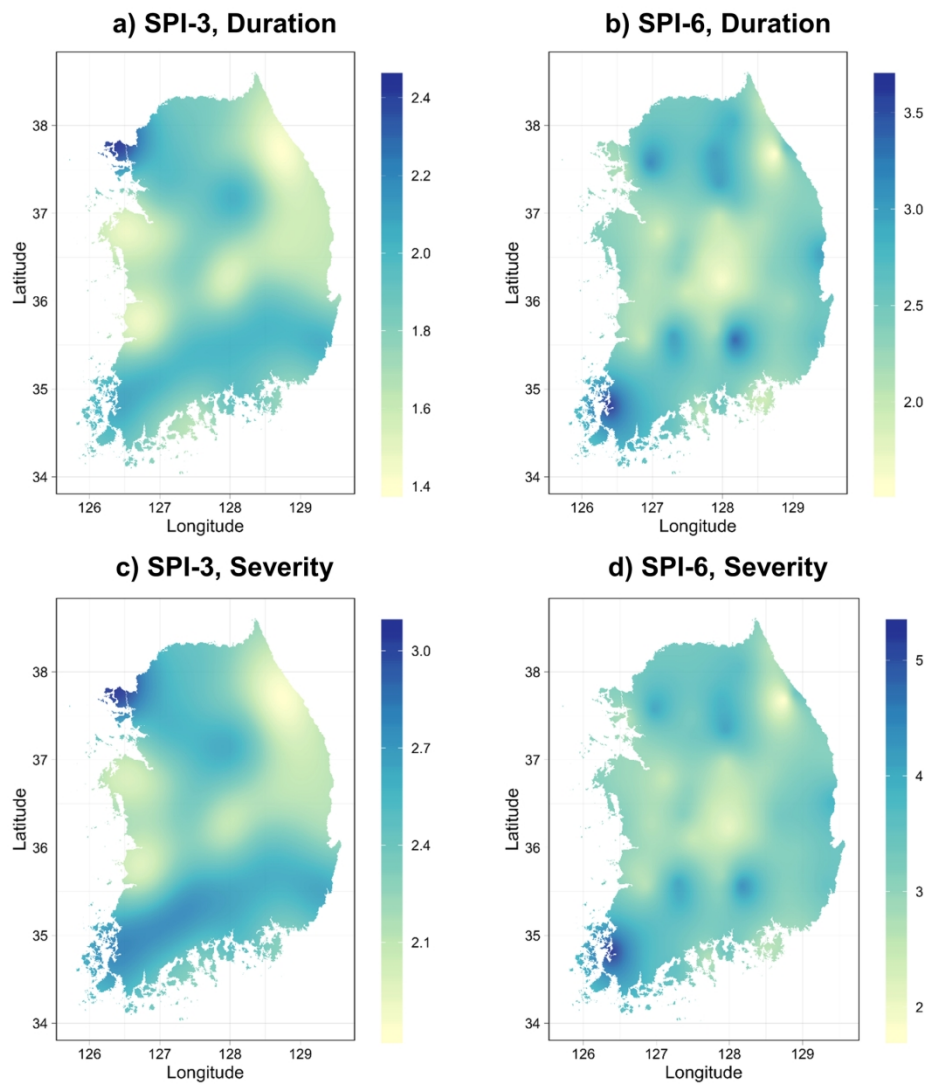
170x189mm (300 x 300 DPI)
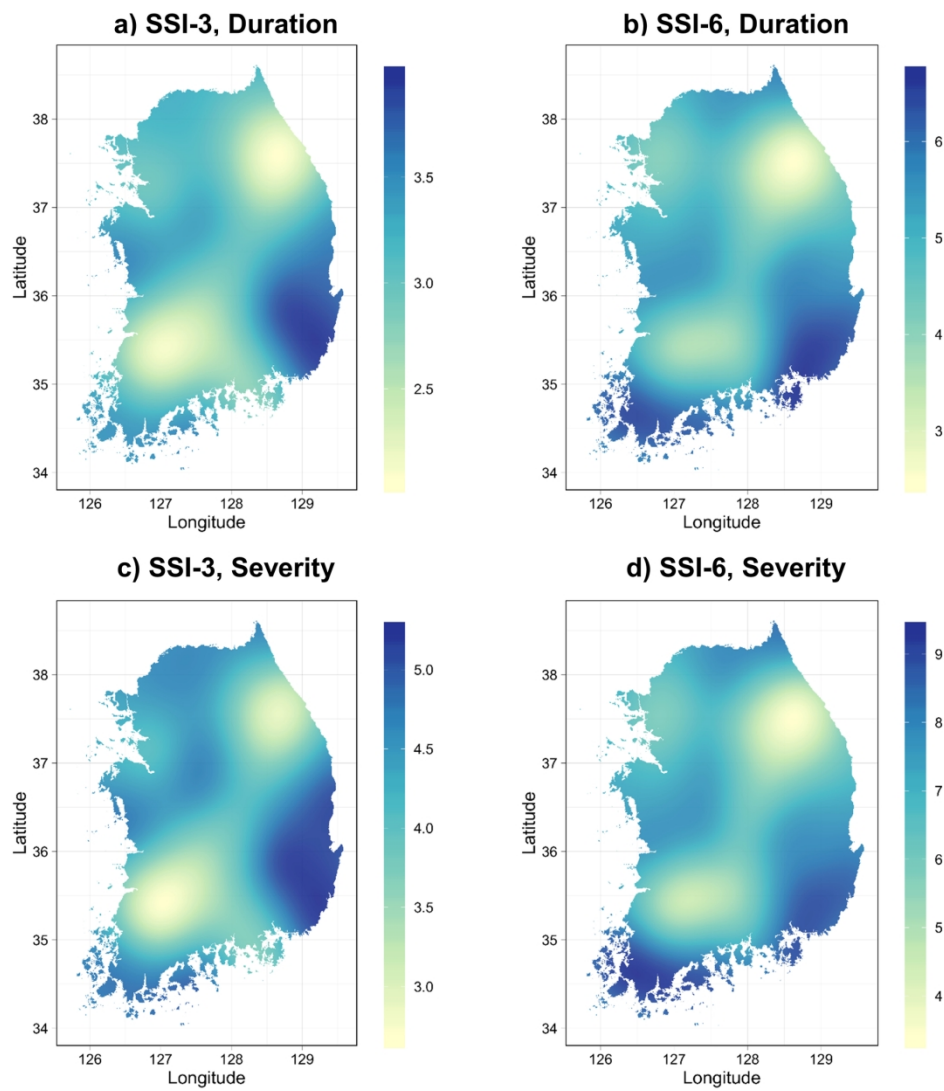
Figure 8. Spatial distribution patterns of agricultural drought (SSI-n) duration and severity using a threshold of -1.0 (moderate drought).

170x189mm (300 x 300 DPI)
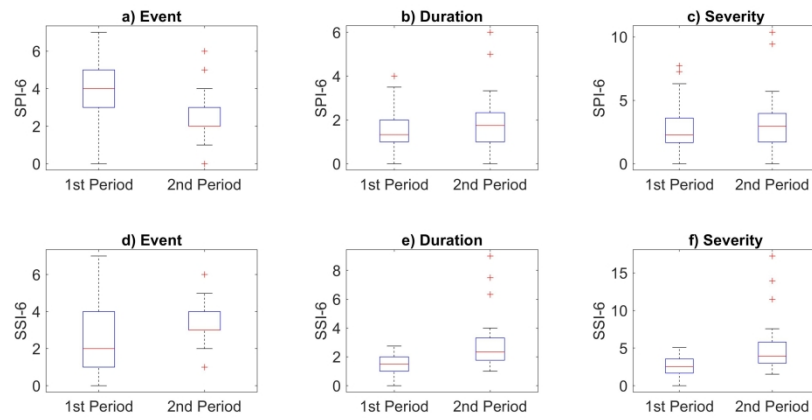
Figure 9. Comparison of drought variables (i.e. frequency, duration and severity) between the first half (1987-2001) and second half (2002-2016) of the period 1987-2016.

344x158mm (300 x 300 DPI)
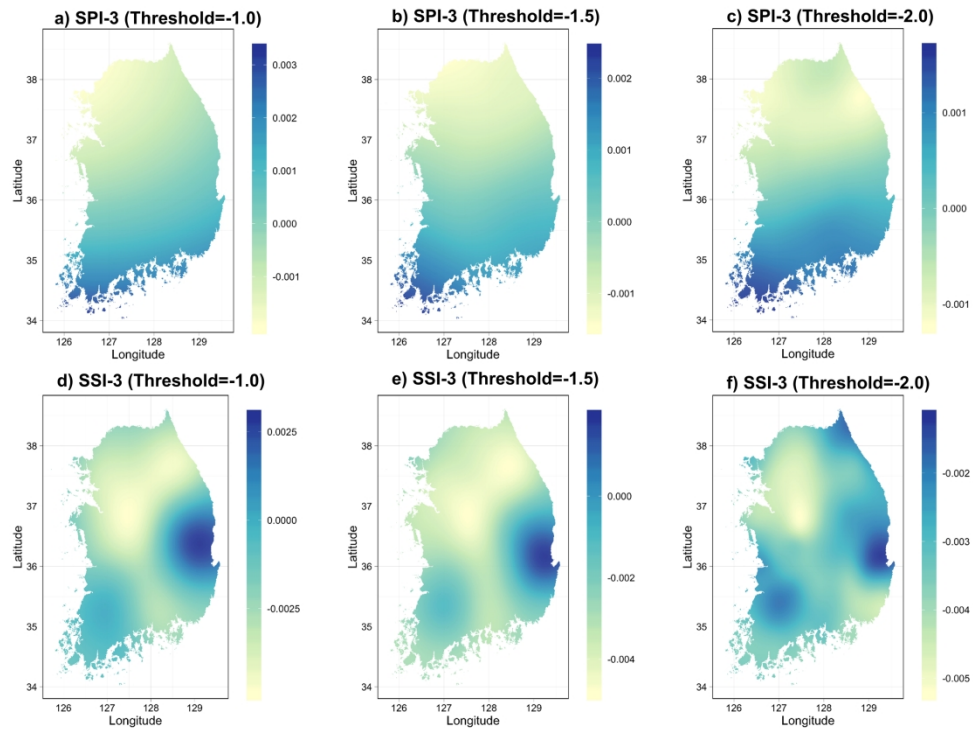
Figure 10. Spatial distribution of trends in SPI-6 and SSI-6 at different quantile levels.

260x190mm (300 x 300 DPI)
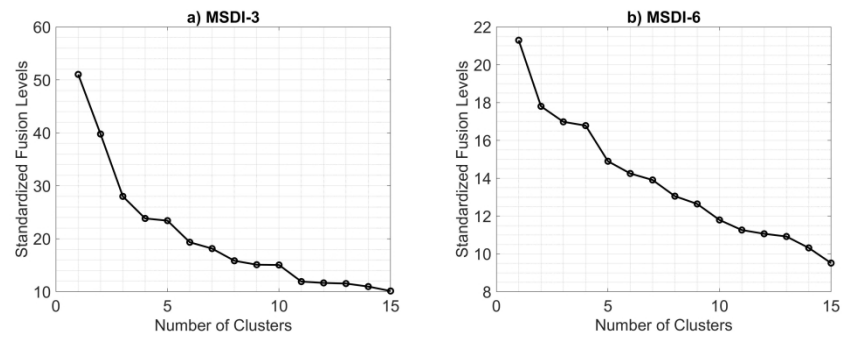
Figure 11. Standardized fusion levels corresponding to the number of clusters for MSDI-3 and MSDI-6.

396x132mm (300 x 300 DPI)
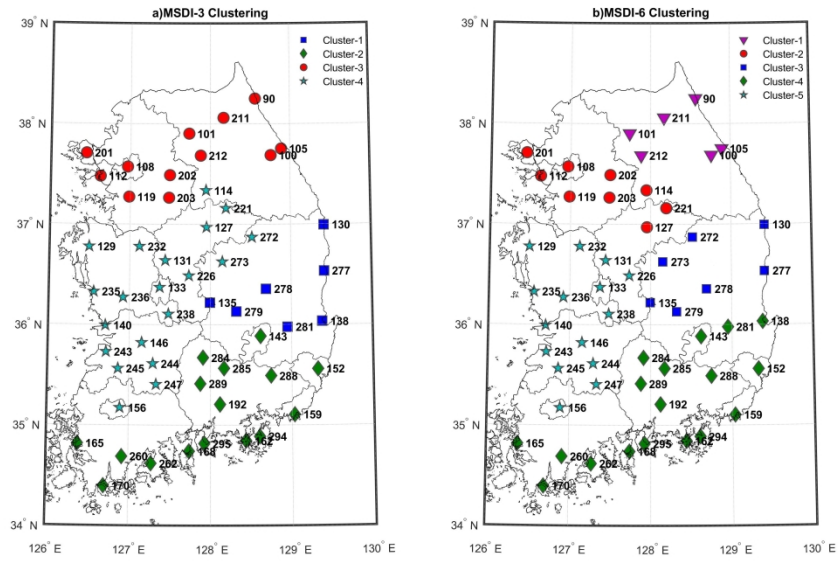
Figure 12. Spatial distribution of clusters for the MSDI over South Korea. Left panel, MSDI-3; right panel, MSDI-6.

317x211mm (300 x 300 DPI)
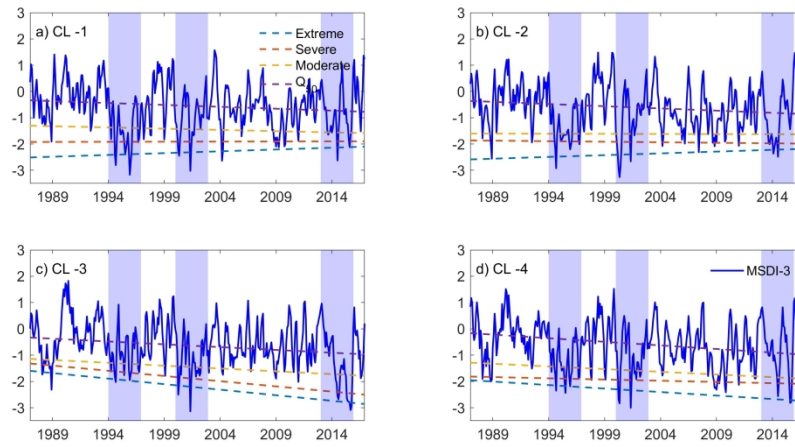
Figure 13. Regional trends of MSDI-3 corresponding to each cluster and their trends over different thresholds based on a quantile regression. Here, blue bars denote three major drought episodes over the past three decades.

317x158mm (300 x 300 DPI)

Figure 14. Regional trends of MSDI-6 corresponding to each cluster and their trends over different thresholds based on a quantile regression. Here, blue bars denote three major drought episodes over the past three decades.

317x246mm (300 x 300 DPI)

Table 1. Rainfall stations used in this study and their annual rainfall.

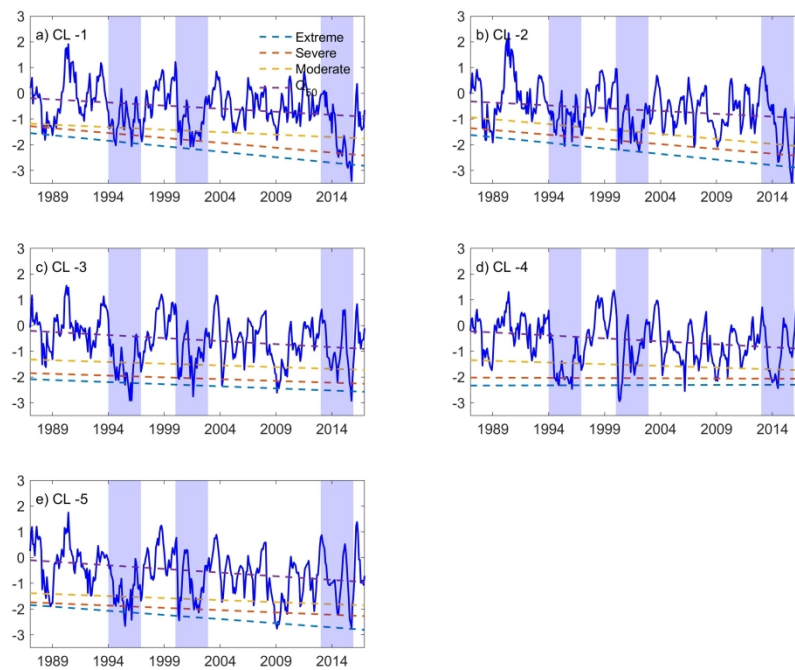| Sta. No	Sta. Name	Lat. (N)	Lon. (E)	Alt. (m)	Annual	NDJ	FMA	MJJ	ASO	Sta. No	Sta. Name	Lat. (N)	Lon. (E)	Alt. (m)	Annual	NDJ	FMA	MJJ	ASO
90	Sokcho	38.25	128.56	18.1	1,386	142	207	653	384	203	Icheon	37.26	127.48	78.0	1,277	109	273	631	264
100	Daegwallyeong	37.69	128.76	772.6	1,765	150	274	897	444	211	Inje	38.06	128.17	200.2	1,394	120	241	786	247
101	Chuncheon	37.90	127.74	76.5	1,356	70	205	850	231	212	Hongcheon	37.68	127.88	140.0	1,520	119	383	757	262
105	Gangneung	37.75	128.89	26.0	1,451	154	222	653	422	221	Jecheon	37.16	128.19	259.8	1,463	113	384	705	260
108	Seoul	37.57	126.97	85.8	1,453	69	214	919	251	226	Boeun	36.49	127.73	175.0	1,163	110	231	595	228
112	Incheon	37.48	126.62	68.2	1,237	64	194	742	238	232	Cheonan	36.78	127.12	81.5	1,445	96	351	750	248
114	Wonju	37.34	127.95	148.6	1,346	73	203	819	252	235	Boryeong	36.33	126.56	15.5	1,536	127	384	737	288
119	Suwon	37.27	126.99	34.1	1,327	73	207	803	244	236	Buyeo	36.27	126.92	11.3	1,524	107	340	803	274
127	Chungju	36.97	127.95	116.3	1,239	75	199	721	244	238	Geumsan	36.11	127.48	170.4	1,337	58	210	818	251
129	Seosan	36.78	126.49	28.9	1,273	91	219	714	249	243	Buan	35.73	126.72	12.0	1,409	68	202	893	246
130	Uljin	36.99	129.41	50.0	1,155	133	197	508	318	244	Imsil	35.61	127.29	247.9	1,361	74	215	810	263
131	Cheongju	36.64	127.44	58.7	1,242	83	203	717	240	245	Jeongeup	35.56	126.87	69.8	1,197	60	189	729	218
133	Daejeon	36.37	127.37	68.9	1,366	97	225	792	252	247	Namwon	35.41	127.33	132.5	1,362	65	209	843	245
135	Chupungnyeong	36.22	127.99	243.7	1,897	136	484	931	346	260	Jangheung	34.69	126.92	45.0	1,412	82	231	847	253
138	Pohang	36.03	129.38	2.3	1,850	144	479	906	322	262	Goheung	34.62	127.28	53.1	1,308	89	219	767	233
140	Gunsan	35.99	126.71	23.2	1,554	97	282	873	302	272	Yeongju	36.87	128.52	210.8	1,238	78	191	718	251
143	Daegu	35.89	128.62	53.5	1,233	80	258	673	222	273	Mungyeong	36.63	128.15	170.6	1,230	93	203	690	244
146	Jeonju	35.82	127.15	61.4	1,298	77	236	747	237	277	Yeongdeok	36.53	129.41	42.1	1,358	97	235	773	254
152	Ulsan	35.56	129.32	83.2	1,309	88	230	744	247	278	Uiseong	36.36	128.69	81.8	1,289	98	220	746	225
156	Gwangju	35.17	126.89	72.4	1,091	68	199	604	220	279	Gumi	36.13	128.32	48.9	1,222	113	211	661	237
159	Busan	35.10	129.03	69.6	1,073	69	210	589	205	281	Yeongcheon	35.98	128.95	93.8	1,352	107	226	774	244
162	Tongyeong	34.85	128.44	32.3	1,078	107	202	505	263	284	Geochang	35.67	127.91	226.0	1,327	124	226	722	254
165	Mokpo	34.82	126.38	38.0	1,015	59	189	576	191	285	Hapcheon	35.57	128.17	32.0	1,348	103	229	772	243
168	Yeosu	34.74	127.74	64.6	1,185	86	210	668	221	288	Miryang	35.49	128.74	11.2	1,485	106	310	804	265
170	Wando	34.40	126.70	35.2	1,183	115	227	562	279	289	Sancheong	35.41	127.88	138.1	1,448	103	355	735	254
192	Jinju	35.21	128.12	30.2	1,243	105	211	688	240	294	Geoje	34.89	128.60	45.4	1,322	75	255	748	244
201	Ganghwa	37.71	126.45	47.0	1,075	68	200	597	210	295	Namhae	34.82	127.93	43.7	1,288	77	241	742	230
202	Yangpyeong	37.49	127.49	48.0	1,293	105	218	740	231										

Table 2. The SPI (SSI) drought severity classification and interpretation.

SPI values	Drought category
≥ 2.0	Extremely wet
1.5 to 1.99	Severely wet
1.0 to 1.49	Moderately wet
0.99 to -0.99	Near normal
-1.0 to -1.49	Moderately dry
-1.5 to -1.99	Severely dry
≤ -2.0	Extremely dry

Table 3. Summary of drought episodes based on clustering analysis.

Threshold	Number of Events					Duration					Severity				
	CL-1	CL-2	CL-3	CL-4	CL-5	CL-1	CL-2	CL-3	CL-4	CL-5	CL-1	CL-2	CL-3	CL-4	CL-5
MSDI-3															
Moderate	33	29	**41**	34		3.4	**4.5**	3.0	3.5		5.5	**7.2**	4.6	5.6	
Severe	22	25	**26**	**26**		2.6	**2.8**	2.2	2.5		5.1	**5.4**	4.2	4.8	
Extreme	11	**13**	7	11		1.8	1.6	**2.3**	1.6		4.4	3.8	**5.8**	3.9	
MSDI-6															
Moderate	**25**	**25**	23	20	24	4.6	4.8	5.2	**6.4**	5.0	7.1	7.6	8.3	**10.3**	8.2
Severe	17	**20**	16	17	19	2.6	2.7	**3.9**	3.8	3.8	5.4	5.3	**7.6**	7.4	7.4
Extreme	7	7	**11**	9	12	3.1	2.7	2.3	**3.3**	2.0	7.5	6.6	5.3	**7.5**	4.7

Table 4. Summary of the slope obtained from a quantile regression model at four different classes. Numbers in bold are statistically significant at the 0.05 level.

Cluster	MSDI-3 ($\times 10^{-3}$)				MSDI-6 ($\times 10^{-3}$)			
	Extreme	**Severe**	**Moderate**	**Q_{50}**	**Extreme**	**Severe**	**Moderate**	**Q_{50}**
CL-1	1.14	0.07	-0.79	-1.21	**-3.55**	**-3.17**	**-1.60**	**-2.00**
CL-2	1.13	-0.34	-0.07	**-1.39**	**-3.63**	**-3.07**	**-3.19**	**-1.82**
CL-3	**-3.51**	**-3.29**	**-1.79**	**-1.78**	-1.36	-1.15	-1.11	**-1.96**
CL-4	**-2.21**	-0.77	**-1.70**	**-2.28**	0.09	-0.13	-1.10	**-1.92**
CL-5					**-2.69**	-1.49	-1.32	**-2.37**

Spatio-temporal drought patterns of multiple drought indices based on precipitation and soil moisture: A case study in South Korea

Moonhyuk Kwon, Hyun-Han Kwon* and Dawei Han

We explore the spatio-temporal characteristics of meteorological and agricultural droughts, respectively, as well as their relationships over the past three decades (1986-2016). Further, the hierarchical agglomerative clustering approach is employed to identify the spatial pattern of the combined drought indices (the SSI and SPI) in South Korea.